JVSTA
JOURNAL OF VACUUM SCIENCE AND TECHNOLOGY A

Study on the oxidation and reduction of tungsten surface for sub-50nm patterning process

Jong Kyu Kim, Seok Woo Nam, Sung Il Cho, Myung S. Jhon, Kyung Suk Min et al.

Citation: J. Vac. Sci. Technol. A **30**, 061305 (2012); doi: 10.1116/1.4758790
View online: http://dx.doi.org/10.1116/1.4758790
View Table of Contents: http://avspublications.org/resource/1/JVTAD6/v30/i6
Published by the AVS: Science & Technology of Materials, Interfaces, and Processing

Study on the oxidation and reduction of tungsten surface for sub-50 nm patterning process

Jong Kyu Kim
Memory Division Semiconductor Business, Samsung Electronics, San No. 16 Banwol-Ri, Taean-Eup, Hwasung-City, Gyeonggi-Do 449-711, South Korea and Department of Advanced Materials Science and Engineering, Sungkyunkwan University, Suwon, Gyeonggi-do 440-746, South Korea

Seok Woo Nam and Sung Il Cho
Memory Division Semiconductor Business, Samsung Electronics, San No. 16 Banwol-Ri, Taean-Eup, Hwasung-City, Gyeonggi-Do 449-711, South Korea

Myung S. Jhon
Department of Chemical Engineering and Data Storage Systems Center, Carnegie Mellon University, Pittsburgh, Pennsylvania 15213

Kyung Suk Min, Chan Kyu Kim, Ho Bum Jung, and Geun Young Yeom[a)]
Department of Advanced Materials Science and Engineering, Sungkyunkwan University, Suwon, Gyeonggi-do 440-746, South Korea

(Received 7 May 2012; accepted 28 September 2012; published 19 October 2012)

The oxidation characteristics of tungsten line pattern during the carbon-based mask-layer removal process using oxygen plasmas have been investigated for sub-50 nm patterning processes, in addition to the reduction characteristics of the WO_x layer formed on the tungsten line surface using hydrogen plasmas. The surface oxidation of tungsten lines during the mask layer removal process could be minimized by using low-temperature (300 K) plasma processing for the removal of the carbon-based material. Using this technique, the thickness of WO_x on the tungsten line could be decreased to 25% compared to results from high-temperature processing. The WO_x layer could also be completely removed at a low temperature of 300 K using a hydrogen plasma by supplying bias power to the tungsten substrate to provide a activation energy for the reduction. When this oxidation and reduction technique was applied to actual 40-nm-CD device processing, the complete removal of WO_x formed on the sidewall of tungsten line could be observed. © *2012 American Vacuum Society*. [http://dx.doi.org/10.1116/1.4758790]

I. INTRODUCTION

In the fabrication of semiconductor and nanoelectronic devices, the pattern pitch used in very large-scale integration (VLSI) circuits has been reduced every year to achieve higher pattern density on the same substrate area.[1,2] One of the serious limitations of high-speed memory devices caused by reducing the pattern sizes is the resistance–capacitance (RC) time delay.[3,4] Particularly, as the pattern width of the word line for memory device is reduced to less than 50 nm, it has been difficult to obtain the electrical properties using the conventional word line based on silicon material due to high resistance.[5,6] To improve the RC time delay, low-resistance conducting materials such as W, Pt, Re, Co, TiN, TaN, etc., have been investigated to replace the amorphous silicon-based word line.[7–10]

Tungsten (W) has the most attention among various materials as the next-generation word line to replace silicon, due to advantage such as high thermal stability, sheet resistance lower than 5 Ω/sq, uniform resistance per area regardless of pattern size, and excellent patterning properties due to the small grain size.[11–14] Other properties required for nanoscale patterning regarding factors such as contamination, morphology, resistance control, surface reaction, and patterning properties have been considered.[11,15] However, the oxidation of tungsten surfaces during processing is a critical problem that needs to be solved for the application of tungsten as the word line for nanoscale semiconductor devices.

In general, tungsten line patterns are formed by masking using a mask layer composed of carbon-based materials such as photoresist (PR) or an amorphous carbon layer (ACL) followed by plasma etching of the tunsten.[16,17] After etching, the carbon-based mask layer is removed at a high temperature by oxygen plasma ashing. During the plasma ashing, the sidewall of the tungsten line pattern is exposed to the oxygen plasma and it is easily oxidized through the diffusion of oxygen species by the thermal activation energy that is reached as a result of the high temperature. Figures 1(a) and 1(b) show a tungsten line before and after the oxygen plasma ashing of the mask layer. A WO_x layer was formed on the sidewall of the tungsten line after the plasma ashing of the mask layer. The WO_x layer formed on the sidewall of tungsten line acts as an insulator, and it increases the resistance of the tungsten line, making it difficult to obtain the tungsten nanoscale pattern size with the required electrical characteristics.

Research on controlling the oxidation of tungsten sidewall patterns has been conducted to minimize the unwanted change of the tungsten pattern surface.[18] Covering the tungsten sidewall with a material to passivate the tungsten surface has been suggested before the mask layer removal using

[a)]Electronic mail: gyyeom@skku.edu

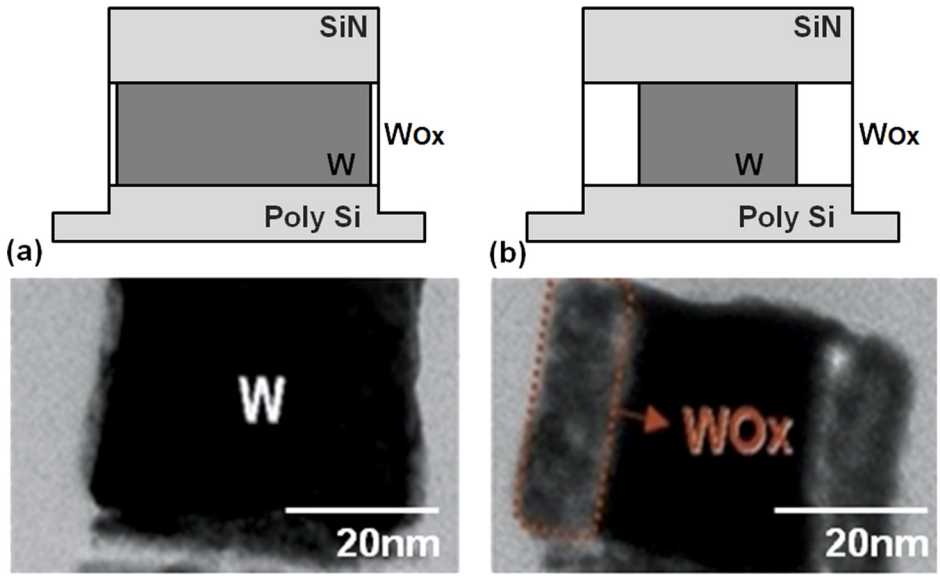

FIG. 1. (Color online) Tungsten line before and after the oxygen plasma ashing of the mask layer for tungsten line pattern at a high temperature (>400 K): (a) before the oxygen plasma ashing and (b) after the oxygen plasma ashing of the mask layer.

oxygen plasmas. The removal of the mask layer or polymeric residue using hydrogen plasmas or nitrogen plasmas instead of oxygen plasmas has also been suggested.[19,20] However, these techniques require additional processes or are known to remove the carbon-based masking layer or polymeric residue ineffectively.[21] Currently, no reports can be found on the minimization of the tungsten sidewall surface oxidation in addition to the effective removal of the carbon-based mask layer by controlling the plasma conditions at a low temperature.

In this study, the degree of tungsten surface oxidation was investigated by varying oxygen plasma conditions to minimize the tungsten surface oxidation. The effect of bias power on the substrate was investigated to control the activation of the mask layer removal at a low temperature during the oxygen plasma ashing using an inductively coupled plasma (ICP) etching system. By controlling the activation of the mask layer removal at a low temperature, we tried to minimize the thermal oxidation of the tungsten sidewall surface while completely removing the carbon-based mask materials. In addition, even though the reaction between the oxygen species in the plasma and tungsten surface is minimized, it is impossible to remove the tungsten surface oxidation completely and a thin WO_x layer is formed. One of the techniques for reducing the thin WO_x layer is to use the reaction between the hydrogen and oxidized surface.[22,23] In general, to reduce the WO_x layer, a high temperature is used to provide the activation energy for the reduction during the exposure to hydrogen species. However, high temperature processing tends to damage the substructure of the VLSI circuit, making the high-temperature processing not easily applicable. Therefore, in this study, a method for reducing the WO_x layer was also investigated at a low temperature by controlling plasma parameters while using hydrogen plasmas. The activation energy for the reduction reaction was also supplied by applying bias power during the hydrogen ICP processing.

II. EXPERIMENT

A microwave plasma-type carbon stripper (Supra3, PSK, Inc.) was used for high-temperature oxygen plasma ashing process. An ICP-type etcher (E-highland, Mattson, Inc.) was employed for the plasma ashing of the mask layer through oxidation and reduction during low-temperature processes. During the plasma processing at low temperature using the ICP, the substrate electrode temperature was set to 300 K. On the substrate, a bias power of 13.56 MHz was introduced in addition to the ICP source power, and the plasma parameters were varied to find an adequate reaction window for the minimization of the tungsten surface oxidation while completely removing carbon-mask layers such as PR, ACL, polymeric layers, and residue. Between the oxidation and the reduction in the same system, the process chamber was seasoned by 900 sccm O_2 gas flow for 2 min followed by 300 sccm N_2 gas flow for 2 min without plasma ignition.

As the samples, 200-nm-thick tetraethylorthosilicate (TEOS) was deposited on bare silicon wafer by chemical vapor deposition followed by the deposition of 35-nm-thick tungsten and 5-nm-thick tungsten nitride sequentially on the TEOS-deposited silicon wafer. To estimate the reactivity between carbon-based materials and oxygen, 3μ-thick KrF PR was deposited on the bare silicon wafer. To investigate the reaction of the tungsten sidewall surface with oxygen and hydrogen in patterned wafers, 40-nm tungsten line pattern composed of a SiN layer, a tungsten layer, and polysilicon was prepared using a PR mask layer.

The tungsten line pattern was treated after oxidation/reduction reaction by a solution of NH_4OH, CH_3COOH, HF, and H_2O which has a selective solubility between tungsten and WO_x. After 10 min of reaction in the solution, the sidewall profile change of the tungsten pattern was investigated. After oxidation and/or reduction plasma processing, the change of WO_x thickness was calculated using x-ray reflectometry (XRR) and scanning ellipsometry (SE). The sheet

resistance (R_s) of the wafer was measured with a four-terminal probe method. X-ray photoelectron spectroscopy (XPS) was used to characterize the change of the tungsten surface after the plasma processing. A transmission electron microscope (TEM) and a scanning electron microscope (SEM) were used to observe the tungsten line pattern profiles and the degree of oxidation of the tungsten sidewall surface in the patterned wafers.

III. RESULTS AND DISCUSSION

A. Oxidation

The oxidation reaction between metal and oxygen molecules requires an activation energy for the reaction. It is believed that even for the reaction between metal and oxygen radicals, an activation energy is required, even though it is small compared to that between metal and oxygen molecules. Figures 2(a) and 2(b) show the sheet resistance change measured as a function of process temperature for 20 s oxidation and the tungsten oxide thickness measured as a function of process time at 300 and 520 K. The oxidation of tungsten shown in Figs. 2(a) and 2(b) was conducted with a microwave plasma-type carbon stripper described in Sec. II. In general, tungsten is oxidized when the tungsten substrate temperature is higher than 400 K. As shown in Fig. 2(a), when the process temperature was higher than 400 K, the R_s of tungsten rapidly increased, indicating the supply of activation energy for tungsten oxidation through the reaction of tungsten with oxygen. Also, as shown in Fig. 2(b), even though the tungsten oxide thickness was increased with time at 520 K due to the continuous reaction of tungsten with oxygen, at the temperature of 300 K, the oxide thickness was nearly saturated at less than 1 nm due to insufficient activation energy for the reaction, even though the activation energy is small.

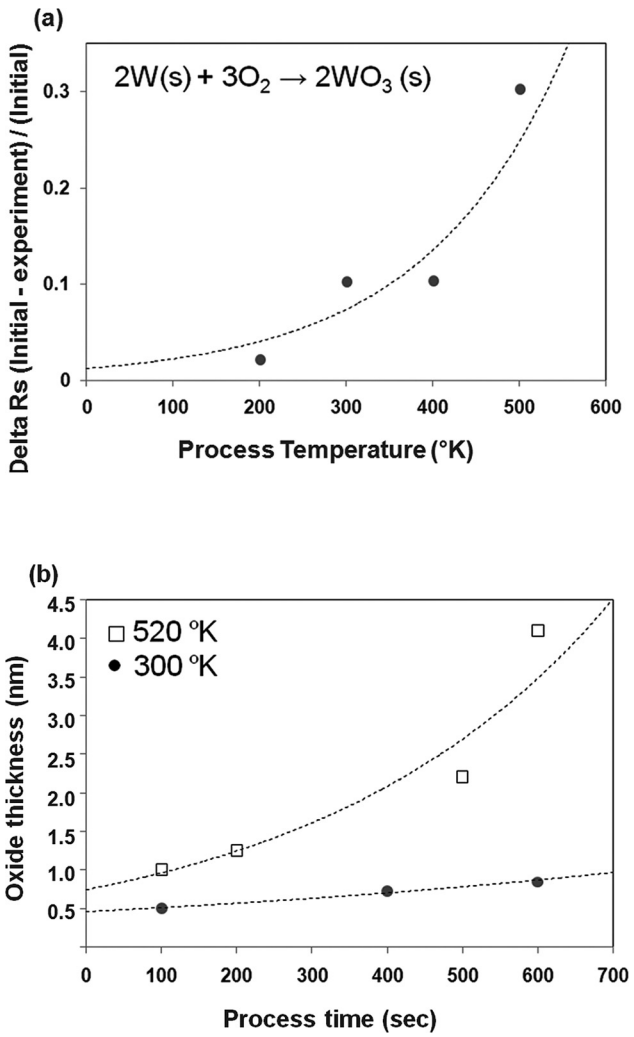

FIG. 2. Surface change of tungsten layer after the exposure to oxygen plasma. (a) The sheet resistance change (delta R_s) measured as a function of process temperature for 20 s of oxidation. (b) The tungsten oxide thickness measured as a function of process time at 300 and 520 K. The oxidation of tungsten was conducted with a microwave plasma-type carbon stripper (4800 W_s, 1 Torr, 9 slm O_2).

At the temperature of 300 K, which is lower than the thermal activation temperature for tungsten oxidation, the degree of tungsten oxidation and PR ashing rate were investigated as a function of process parameters using an ICP-type etching system described in Sec. II. Here, the PR ashing rate represents the removal rate of carbon-based materials such as polymeric residue, carbon-based hardmask material, etc. In this experiment, bias power was introduced in addition to source power as a parameter for WO_x formation. Figures 3(a)–3(c) show the effect of bias power, source power, and total flow rate on the PR ashing rate and the thickness of WO_x formed on the tungsten surface, respectively. The oxygen pressure was maintained at 15 mTorr, and the processing time was 20 s. When one of the parameters was varied, the source power, bias power, and total flow rate were maintained at 1800 W_s, 100 W_b, and 900 sccm, respectively. In the figures, there was some variation of data values for the same processing condition of Figs. 3(a)–3(c) during each set of experiments, which was possibly due to slight changes in the chamber conditions; however, the trend was the same. The WO_x thickness was measured by XRR and the PR ashing rate was measured by SE. As shown in Figure 3(a), even though the experiment was carried out at 300 K, a temperature lower than the thermal activation energy, the WO_x thickness increased almost linearly with the bias power. The WO_x thickness at 500 W_b was about four times higher than that at 100 W_b. Therefore, even though the thermal activation energy was not supplied by the substrate temperature, the reaction between tungsten and oxygen can be promoted by the bias power in the form of ion bombardment energy. However, when the source power was increased while maintaining the bias power at 100 W_b, as shown in Fig. 3(b), the WO_x thickness did not vary significantly due to the negligible change in the activation energy for WO_x formation. In fact, the thickness of WO_x slightly decreased with the increase of source power, which was possibly due to the slight decrease of the ion bombardment energy (V_{dc}) with the increase of source power at a fixed bias power. As shown in Fig. 3(c), the increase of total flow rate did not change the WO_x thickness significantly due to the lack of change in the ion bombardment energy at a given operating pressure. Therefore, the WO_x formation was not affected by the reactant concentration at low thermal/ion bombardment energy

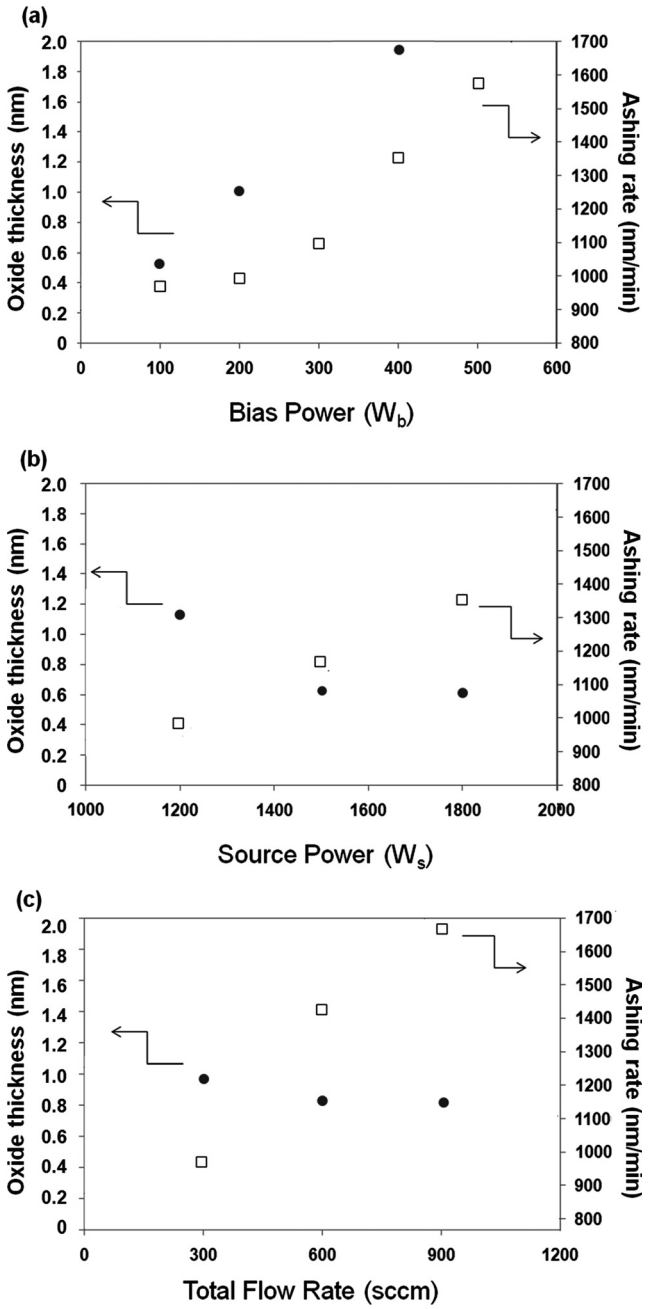

FIG. 3. Effect of (a) bias power, (b) source power, and (c) total oxygen flow rate on the PR ashing rate and the thickness of WO_x formed on tungsten surface at a low temperature (300 K). The oxygen pressure was maintained at 15 mTorr, and the processing time was 20 s. When one of the parameters was varied, the parameters such as source power, bias power, and total flow rate were maintained at 1800 W_s, 100 W_b, and 900 sccm, respectively.

conditions because the activation energy is the limiting factor for the WO_x formation.

As shown in Fig. 3(a), the PR ashing rate increased with the increase of bias power, similarly to the trend in WO_x thickness, due to the increase of reaction rate between carbon-based material and oxygen through the ion bombardment. However, as shown in Figs. 3(b) and 3(c), the PR ashing rate was also increased with the increase of source power and total flow rate. The reaction between carbon-based material and oxygen does not require high activation energy. Therefore, the ashing rate was increased not only with the increase of ion bombardment energy but also with the increase of reactant concentration at low thermal/ion bombardment energy conditions because the activation energy for the PR ashing reaction is not the limiting factor for the reaction. When oxygen radicals do not react with the substrate, the oxygen radical concentration is decreased with the increase of oxygen flow rate at the same operating pressure due to the decreased residence time. However, when the reactants react with the substrates, due to the reaction of oxygen radicals and by the formation of etch by-products, the oxygen radical concentration is increased with the increase of oxygen gas flow rate, as seen with the increase of ashing rate with the increase of oxygen flow rate. Using the differences in the activation energy between WO_x formation and PR ashing (or the removal rate of carbon-based materials), the WO_x thickness can be minimized while the carbon-based mask material and polymeric residue on the tungsten line pattern are removed effectively.

The process conditions which minimize the oxidation of tungsten while effectively removing the carbon-based mask layer were applied to the 40-nm tungsten line patterning process. Figures 4(a) and 4(b) show the WO_x thickness after a conventional high-temperature mask removal processing (520 K) using the microwave carbon stripper and that after the optimized low-temperature (300 K) processing using the ICP etching system, respectively. For the low-temperature processing, to minimize the formation of WO_x while increasing the oxidation reaction of carbon-based material, high-density plasma was used without applying bias power to the ICP etcher. As shown in the figure, the WO_x thickness was decreased by 25% as a result of using the low temperature processing instead of the conventional high-temperature processing (the measured thicknesses of WO_x in Figs. 3 and 4 were somewhat different due to the different measurement tools used). The same processes were applied to the 40-nm tungsten line pattern processing, and the results are shown in Figs. 4(c) and 4(d) after the high-temperature processing and after the low-temperature processing, respectively. The patterned wafer was treated in a solution of NH_4OH, CH_3COOH, HF, and H_2O for 10 min after the oxygen plasma ashing to remove the WO_x layer formed on the tungsten line surface. As shown, after the removal of the WO_x layer, the tungsten line width decreased for the high-temperature processing due to the formation of thick WO_x on the sidewall of the tungsten line pattern. However, when the low-temperature processing was used, the tungsten line pattern was not decreased significantly due to very thin WO_x formation on the sidewall of the tungsten line. However, as shown in Figs. 4(b) and 4(d), even though the activation energy was not supplied by not applying bias power during the ICP-type plasma ashing, the tungsten surface reacted with oxygen and formed thin WO_x on the surface. This was possibly due to the oxygen ion bombardment by the sheath potential close to the plasma potential or by the high-energy tail of the Maxwellian distribution of oxygen species. Therefore, even though the WO_x formation can be minimized by control of the thermal/ion bombardment energy, it is not possible to remove the WO_x formation completely during the plasma ashing. To remove the WO_x layer that formed on the tungsten during the plasma ashing, a reduction process has

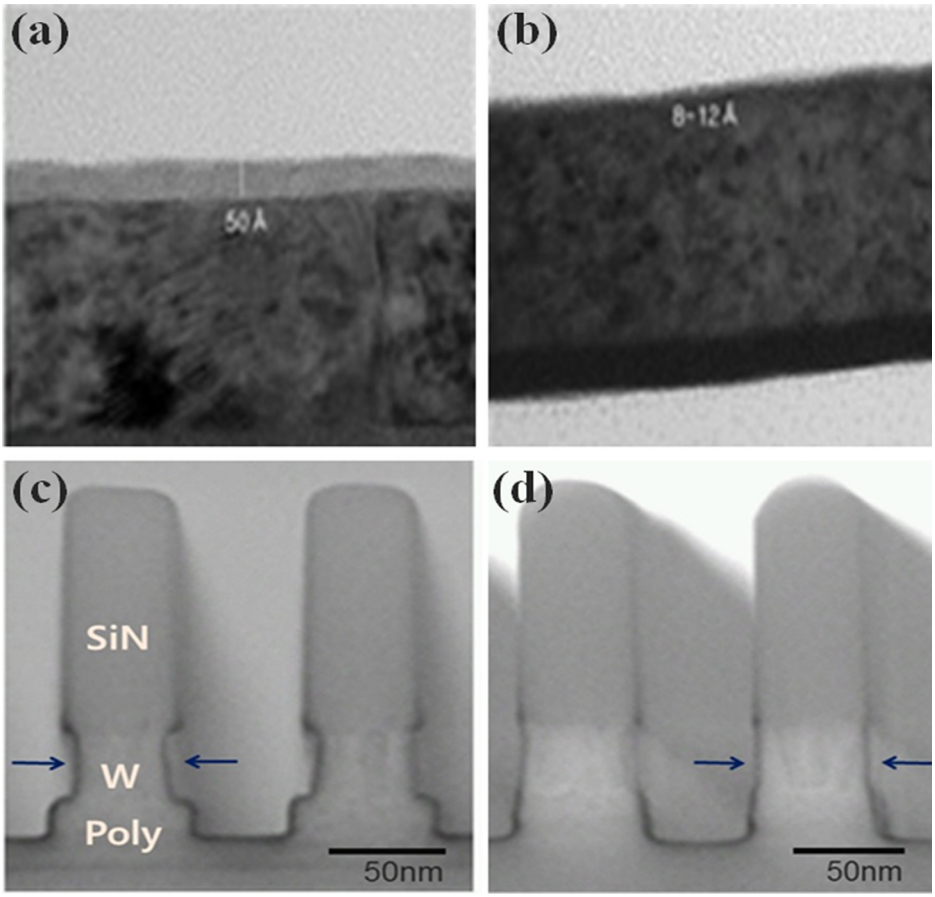

FIG. 4. (Color online) Comparison of tungsten surface oxidation after the mask layer removal processing at different process temperatures. (Patterned wafer was treated in a solution, a mixture of NH_4OH, CH_3COOH, HF, and H_2O, for 10 min). (a) Bare tungsten wafer after a high temperature plasma processing. (b) Bare tungsten wafer at a low-temperature plasma processing. (c) Patterned wafer at a high-temperature plasma processing. (d) Patterned wafer after a low temperature plasma processing. (a) and (c) were processed at 520 K using the microwave plasma system at the condition of 4800 Ws, 1 Torr, 9 slm of O_2, and for 20 s. (b) and (d) were processed at 300 K using the ICP system at the condition of 1800 W_s, 15 mTorr, 900 sccm of O_2 for 20 s.

been investigated in addition to the study on the minimization of the WO_x formation.

B. Reduction

The reduction reaction that forms tungsten and H_2O as a byproduct from the reaction of WO_x with hydrogen is thermodynamically favorable if the required activation energy is provided for the initiation of the process similar to the oxidation case.[24] In general, for the reduction of the WO_x, thermal energy is provided to supply the required activation energy. However, this method could cause thermal damage to the nanoscale semiconductor device circuit due to high activation temperature. Therefore, similar to the oxidation case, as a replacement for thermal energy for the activation, bias power was applied to the substrate for the reduction of WO_x to tungsten at a low temperature to avoid thermal damage.

Table I shows the WO_x thickness remaining on the tungsten substrate after the reduction by varying bias power and operating pressure conditions. For the reduction process, the ICP system was also used, and the wafer was processed with 800 W_s of source power, 300 sccm of H_2 flow, and for 30 s at a low temperature (300 K). To estimate the remaining WO_x thickness, XRR and SE were used, and the sheet resistance R_s was measured using a four-point probe after the reduction process. As shown in the table, the thickness of WO_x estimated by XRR and SE decreased with the increase of bias power, and the R_s of the tungsten layer also decreased with the increase of bias power due to the decrease of WO_x on the tungsten surface. Similar to the oxidation case in Fig. 4(b), even without applying bias power, the WO_x was slightly reduced by the source plasma itself. When the operating pressure was increased at a fixed bias power, due to the decease of ion bombardment energy caused by the decreased

TABLE I. WO_x thickness remaining on tungsten substrate after the reduction by varying bias power and operating pressure. For the reduction process, an ICP system was used and the wafer was processed with 800 W_s, 15 mTorr, 300 sccm of H2, and for 30 s at a low temperature (300 K).

Bias power	Pressure (mT)	WO_x thickness (nm) by SE	WO_x thickness (nm) by XRR	R_s (Ω cm) by four point probe
Reference		9.17	9.11	6.055
0 W_b	15	9.07	8.37	5.935
150 W_b	15	6.49	6.06	5.781
250 W_b	15	4.58	4.68	5.621
100 W_b	15	8.54	8.72	5.810
100 W_b	25	8.58	8.75	5.843
100 W_b	35	8.71	8.92	5.872

mean free path, the reduction thickness was decreased and R_s was slightly increased. Therefore, it is found that, similar to the oxidation reaction, the WO_x obtains enough activation energy for the reduction process by applying bias powers to the substrate at a low temperature, and the ion bombardment energy is the limiting factor for the WO_x reduction process at low temperature.

Figures 5(a) and 5(b) show the XPS narrow scan data of W and O, respectively, after the oxidation of tungsten (i), after the reduction with 150 W_b of bias power (ii), and after the reduction with 300 W_b of bias power (iii). The wafer was processed with 800 W_s, 15 mTorr, and 300 sccm of H_2 for 30 s at 300 K. As shown in Fig. 5, after the hydrogen reduction by the application of bias power, the peaks related to WO_x and oxygen decreased significantly, and the peak related to metallic tungsten increased significantly. Also, the peak change was more significant at higher bias power, indicating further reduction at this condition. Therefore, the reduction of WO_x by the ion bombardment during the hydrogen plasma processing at low temperature could also be confirmed by XPS analysis.

Figure 6 shows the cross-sectional SEM images of the 40-nm tungsten line pattern (a) after the oxidation of tungsten and (b) after the reduction with bias power after the oxidation with an optimized reduction process 700 W_s, 170 W_b, 15 mTorr, 300 sccm of H_2 flow rate, and for 30 s using the ICP. The tungsten line pattern was treated for 10 min in a solution after the plasma processing. The oxidation of tungsten was processed with the conditions in Fig. 4(b), which reduces the WO_x thickness to 25% of that resulting from the high temperature process. As shown, during the mask layer removal processing, due to the formation of thin WO_x on the tungsten line sidewall, the tungsten line is slightly reduced after the solution treatment. However, as shown in Fig. 6(b), after the reduction of WO_x formed during the oxidation process of (a), no change in the width of the tungsten line pattern was observed after the solution treatment, indicating the complete reduction of WO_x formed on the sidewall of tungsten. The sidewall of tungsten line cannot be directly bombarded by incident ions because the sidewall of the tungsten line is parallel to the direction of bombarding ions. However, as shown in Figs. 4 and 6, even without direct ion bombardment, the sidewall of tungsten was oxidized and reduced. It is believed that, even without the direct bombardment, the sidewall of tungsten can be indirectly bombarded by ions scattered on the mask underlayer (the patterned SiN layer after the removal of the PR mask layer).

To identify the possibility of scattering of the incident ions at the sidewall of the mask underlayer, the change of mask underlayer shape with the increase of bias power was

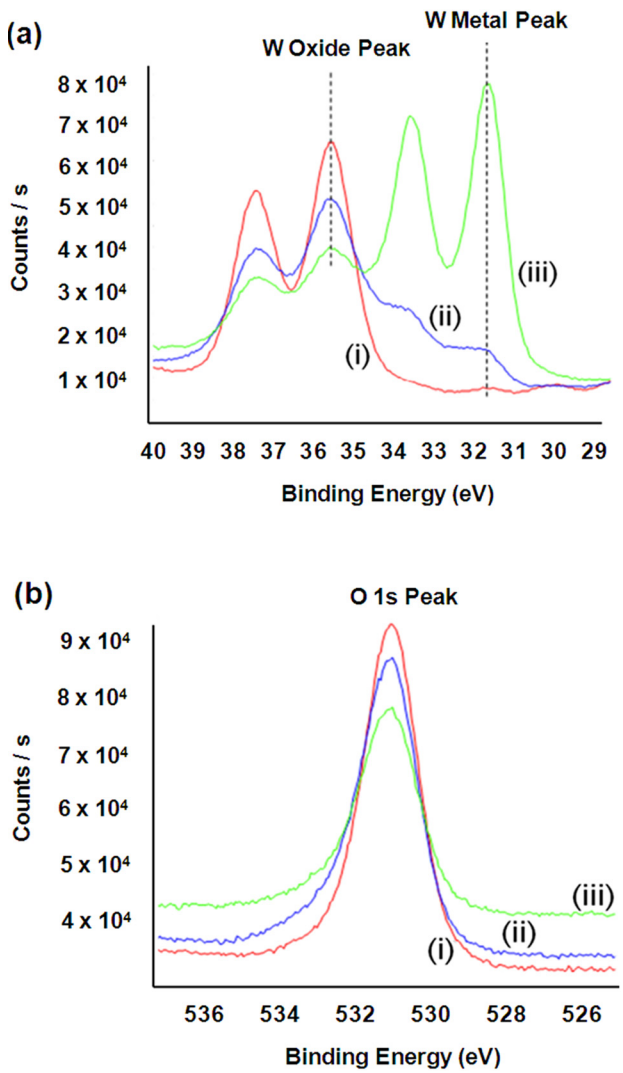

FIG. 5. (Color online) XPS narrow scan data of (a) W and (b) O after the oxidation of tungsten (i), after the reduction with 150 W_b of bias power (ii), and after the reduction with 300 W_b of bias power (iii). The wafer was processed with 800 W_s, 15 m Torr, 300 sccm of H_2, and for 30 s at 300 K using the ICP.

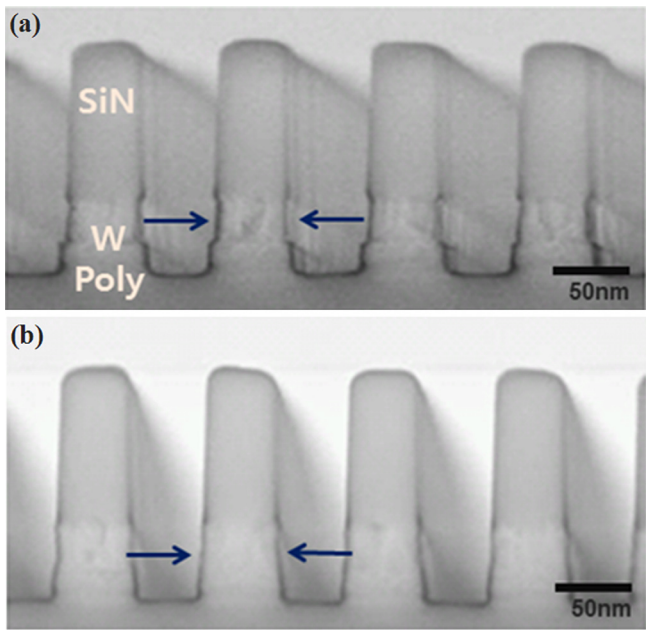

FIG. 6. (Color online) Cross-sectional SEM images of tungsten line pattern (a) after the oxidation of tungsten and (b) after the reduction with a bias power after the oxidation. The tungsten line pattern was treated for 10 min in a solution (a mixture of NH_4OH, CH_3COOH, HF, and H_2O) after the plasma processing.

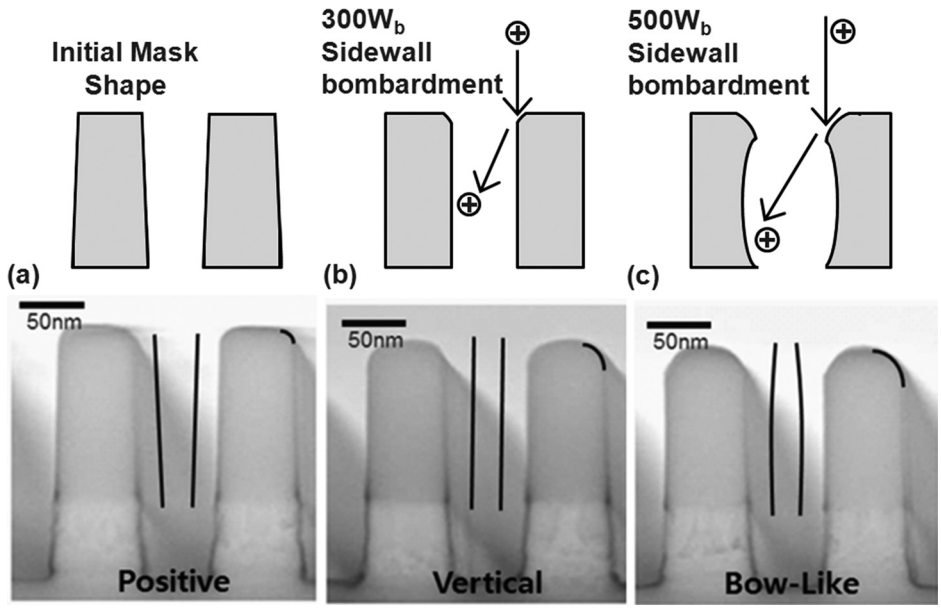

FIG. 7. Erosion and profile change of the mask underlayer with bias power (a) before the reduction, (b) after the reduction with 300 W_b of bias power, and (c) after the reduction with 500 W_b of bias power. Other process conditions are the same as those in Fig. 5.

investigated using SEM, and the results are shown in Fig. 7. As the bias power is increased at the reduction step, the top portion of the mask underlayer is degraded further due to the increase of the incident ions energy. In addition, the mask underlayer profile was also varied with the increase of bias power from a positive slope to a bow-like profile, possibly due to the bombardment of the ions scattered on the top portion of the mask underlayer. Therefore, it is believed that the sidewall of the tungsten line pattern can be bombarded by ions scattered on the mask underlayer, obtaining enough activation energy for the oxidation or reduction described above, at low temperature.

IV. CONCLUSION

A method in minimizing the oxidation of a tungsten line pattern during the carbon-based mask layer removal process and a method for removing the WO_x layer formed on the tungsten line surface by the reduction using hydrogen plasma at a low temperature have been investigated for sub-50 nm semiconductor IC processes. The energy required for the activation of the oxidation or reduction of tungsten was supplied not by thermal energy but by ion bombardment through the bias power to the substrate during the operation of the ICP system. By the optimization of the plasma ashing process at low temperature, which uses a high source power without biasing the substrate, the oxidation of tungsten line patterns could be reduced to 25% of that processed at high temperature while removing the carbon-based mask layer and polymeric residue effectively. The thin WO_x formed during the plasma ashing could be effectively reduced by using hydrogen plasma at a low temperature, again by applying bias power to the substrate instead of using a high temperature. When this low-temperature oxidation and reduction technique was applied to an actual 40-nm-CD tungsten line patterning process, the complete removal of WO_x formed on the sidewall of tungsten line could be observed.

ACKNOWLEDGMENTS

This work was supported by the National Research Foundation of Korea Grant funded by the Korean Government (MEST) (NRF-2010-M1AWA001-2010-0026248) and by the World Class University program of the National Research Foundation of Korea (Grant No. R32-10124). This work was supported by the MKE/KOTEF through the Human Resource Training Project for Strategic Technology.

[1]T. Skotnicki *et al.*, IEEE Trans. Electron Devices **55**, 96 (2008).
[2]R. F. Pease and S. Y. Chou, Proc. IEEE **96**, 248 (2008).
[3]See www.itrs.org for International Technology Roadmap for Semiconductors (2009).
[4]T. Hiramoto, T. Mizutani, A. Kumar, A. Nishida, T. Tsunomura, S. Inaba, K. Takeuchi, S. Kamohara, and T. Mogami, *IEEE International SOI Conference* (2010), p. 170.
[5]K. Kim, Tech. Dig. - Int. Electron Devices Meet. **2010**, 1.
[6]N. J. Son, Y. Oh, W. Kim, W. M. Jang, W. Yang, G. Jin, and K. Kim, IEEE Trans. Electron Devices **51**, 1644 (2004).
[7]E. P. Gusev, V. Narayanan, and M. M. Frank, IBM J. Res. Dev. **50**, 387 (2006).
[8]S. B. Samavedam *et al.*, Tech. Dig. - Int. Electron Devices Meet. **2002**, 433.
[9]J. K. Schaeffer *et al.*, Tech. Dig. - Int. Electron Devices Meet. **2004**, 287.
[10]K. Endo, S. I. O'uchi, Y. Ishikawa, Y. Liu, T. Matsukawa, K. Sakamoto, J. Tsukada, H. Yamauchi, and M. Masahara, IEEE Electron Device Lett. **31**, 546 (2010).
[11]Y. Akasaka, S. Suehiro, K. Nakajima, T. Nakasugi, K. Miyano, and K. Kasai, IEEE Trans. Electron Devices **43**, 1864 (1996).
[12]T. Yamamshita, Y. Nishida, K. Hayasi, T. Eimori, M. Inuishi, and Y. Ohji, Jpn. J. Appl. Phys., Part 1 **43**, 1799 (2004).
[13]M. G. Sung *et al.*, Jpn. J. Appl. Phys., Part 1 **46**, 2134 (2007).
[14]P. B. Shim, J. H. Choy, G. S. Gil, K. M. Kyung, and J. C. Park, J. Electron. Mater. **31**, 988 (2002).
[15]Y. S. Kim, M. G. Sung, and S. K. Park, Solid State Electron. **54**, 650 (2010).
[16]K. Babich *et al.*, Proc. SPIE. **5039**, 152 (2003).

[17]N. A. Hastas, C. A. Dimitriadis, Y. Panayiotatos, D. H. Tassis, S. Logothetidis, D. Papadimitriou, G. Roupakas, and G. Adamopoulos, Semicond. Sci. Technol. **17**, 662 (2002).
[18]C. H. Ho, E. K. Lai, M. D. Lee, C. L. Pan, Y. D. Yao, K. Y. Hsieh, R. Liu, and C. Y. Lu, *IEEE Symposium on VLSI Technology* (2007), p. 228.
[19]S. B. Kim, H. T. Seo, J. K. Song, Y. D. Kim, S. Hyun, Y. C. Kim, and H. T. Jeon, J. Appl. Phys. **42**, 1212 (2003).
[20]X. Hua *et al.*, J. Vac. Sci. Technol. B **24**, 1238 (2006).
[21]D. S. Venables and M. E. Brown, Thermochim. Acta **285**, 361 (1996).
[22]G. J. Stueber, G. Oehrlein, P. Lazzeri, M. Bersani, M. Anderle, E. Busch, and R. McGowan, J. Vac. Sci. Technol. B **25**, 1593 (2007).
[23]X. Wan, D. Goberman, L. L. Shaw, G. Yi, and G. M. Chow, Appl. Phys. Lett. **96**, 123108 (2010).
[24]T. Toda, H. Igarashi, H. Uchida, and M. Watanabe, J. Electrochem. Soc. **146**, 3750 (1999).